

A multi-particle model of the 3C 48 host

J. Scharwächter¹, A. Eckart¹, S. Pfalzner¹, J. Zuther¹, M. Krips^{1,2}, and C. Straubmeier¹

¹ I. Physikalisches Institut, Universität zu Köln, Zùlpicher Str. 77, 50937 Köln

² IRAM, 300, rue de la Piscine, Domaine Universitaire, 38406 Saint Martin d'Hères

Received (date); accepted (date)

Abstract. The first successful multi-particle model for the host of the well-known quasi-stellar object (QSO) 3C 48 is reported. It shows that the morphology and the stellar velocity field of the 3C 48 host can be reproduced by the merger of two disk galaxies. The conditions of the interaction are similar to those used for interpreting the appearance of the "Antennae" (NGC 4038/39) but seen from a different viewing angle. The model supports the controversial hypothesis that 3C 48A is the second nucleus of a merging galaxy, and it suggests a simple solution for the problem of the missing counter tidal tail.

Key words. Galaxies: interactions – Methods: simulations – Quasars: individual: 3C 48

1. Introduction

3C 48 (Barkhouse & Hall 2001) was the first QSO to be discovered optically (Matthews et al. 1961; Matthews & Sandage 1963) and the first QSO to be directly identified with a host galaxy (Boroson & Oke 1982). Its basic properties are listed in Table 1. 3C 48 has attracted much attention regarding the proposed evolutionary sequence of active nuclei (Sanders et al. 1988). According to this scheme, interactions and mergers of galaxies trigger an evolution via ultra-luminous infrared galaxies (ULIRGs) to QSOs. The observational evidence, however, is hampered by the fact that many transitional objects show only dubious indications of past or recent mergers. Clarification requires detailed multi-particle modeling which helps with disentangling the complex spatial structure of merger remnants.

3C 48 is an example of a transitional object with prototypical properties in many respects: It has the typical far-infrared excess, originating from thermal radiation of dust which is heated by the quasar nucleus and by newly forming stars in the host galaxy (Neugebauer et al. 1985; Stockton & Ridgway 1991). Large amounts of molecular gas (Scoville et al. 1993; Wink et al. 1997) indicate the possibility of a young stellar population in the host. Finally, long-slit spectroscopy gives evidence for an ongoing starburst in the host which currently seems to be close to its maximum activity (Canalizo & Stockton 2000). But the merger scenario for 3C 48 is still unclear: Indeed, the host has a significant tail-like extension to the northwest whose tidal origin is rather compelling with regard to the kinematics and ages of its stars (Canalizo & Stockton 2000). However, the nature of the apparent second nucleus 3C 48A about 1'' northeast of the QSO (Stockton & Ridgway 1991) and the location of the expected counter tidal tail remain an unsolved problem. 3C 48A could as well be due to the radio jet (Wilkinson et al. 1991) interacting with the dense interstellar medium (Chatzichristou et al. 1999). A feature at the southeast of the 3C 48 host, previously interpreted as a counter tidal tail (Boyce et al. 1999), has turned out to be a background galaxy (Canalizo & Stockton 2000). Instead, a counter tail extending from the southeast to the southwest is suspected (Canalizo & Stockton 2000) but not yet identified. Canalizo & Stockton (2000) suggest that such a location of the two tidal tails might be explicable by a certain projection of the merger scenario used to simulate the "Antennae".

This paper reports the first successful multi-particle model for the 3C 48 host. Suggesting simple solutions for the 3C 48A problem and the counter tail problem, the model largely resolves doubts about the merger hypothesis for 3C 48.

Send offprint requests to: J. Scharwächter, e-mail: scharw@ph1.uni-koeln.de

Table 1. Basic properties of 3C 48.

RA ₂₀₀₀	01h37m41.3s	Ma et al. (1998)
Dec ₂₀₀₀	+33d09'35"1	Ma et al. (1998)
Redshift	0.367	Barkhouse & Hall (2001)
Luminosity Distance	1,581 Mpc ^a	
Angular Size Distance	846 Mpc ^a	
Scaling Factor	1'' ≈ 4.1 kpc	

^a $H_0 = 75 \text{ km s}^{-1} \text{ Mpc}^{-1}$ and $q_0 = 0.5$ will be adopted throughout the paper.

2. Methods

2.1. Numerical simulations

The stellar-dynamical 3-dimensional N-body simulations are performed with TREESPH (Hernquist & Katz 1989), a tree code used in its non-collisional mode. Stable initial particle distributions for the model galaxies are set up with BUILDGAL (see Hernquist 1993). The spatial orientation of the two disk galaxies is parameterized by their inclinations i with respect to the orbital plane and their pericentric arguments ω as introduced by Toomre & Toomre (1972). Both galaxies have extended mass distributions so that the orbit of their encounter is not Keplerian but decaying. Two descriptions can be used to characterize these orbits: The first one is a pseudo-Keplerian description using the parameters of eccentricity e , pericentric distance r_{peri} , and angle to pericentre Ω_{peri} of the corresponding Keplerian orbit for which the total mass of each galaxy is associated with a point mass at the respective centre of mass. The second one is a direct description of the decaying orbit using the true apocentric and pericentric distances r_{apo} and r_{peri} of the first passage to define an eccentricity in its generalized formulation $e = (r_{\text{apo}} - r_{\text{peri}})/(r_{\text{apo}} + r_{\text{peri}})$. For convenience, the system of units, which remains intrinsically scale-free, is scaled to the system suitable for 3C 48.

The results of the simulations are analyzed as 2-dimensional projections. In order to mock the pixel array data of imaging observations, the particles are sorted into a 512×512 grid. The virtual pixel values are computed by adding up all particles located in a grid cell along the line-of-sight. Without any special weighting of a nuclear component, the mock images are comparable to QSO-subtracted images of the 3C 48 host. Spectra for each grid cell are generated by sorting the particles into velocity channels according to their respective line-of-sight velocities. Thus, an average stellar line-of-sight velocity is assigned to each virtual pixel. The resulting data arrays are spatially smoothed by Gaussian convolution and converted into FITS format to facilitate the further data processing with standard astronomical software.

2.2. Observational data on 3C 48

The data presented by Canalizo & Stockton (2000) are used for comparing the simulations with observations. They provide information about the optical surface-brightness of the QSO-subtracted 3C 48 host (Fig. 1 therein) and about the stellar kinematics along the four slits A, B, C, G (Fig. 1 and Table 2 therein). In reference to these data, the basic proportions of the main body of the 3C 48 host are classified by dimensionless length ratios (left panel of Fig. 1 and left column of Table 3). Such a comparison is independent of the length scaling, in contrast to the comparison of line-of-sight velocities which requires a positioning of the four slits on the mock image. Having determined the final physical length unit of the simulations, the curvature of the northwestern tidal tail is compared by using an angle-versus-distance plot (right panel of Fig. 1 and Fig. 5).

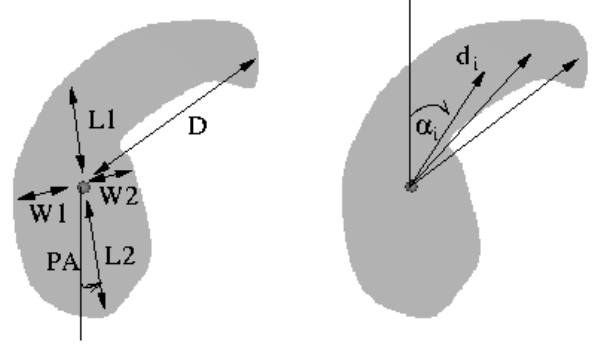


Fig. 1. Sketch of the parameters used for characterizing the dimensions of the 3C 48 host. The lengths ($L1$, $L2$) are measured along the longest extension of the host body ($PA \approx 4^\circ$ for the observations, $PA \approx 19^\circ$ for the simulations), the widths ($W1$, $W2$) are measured perpendicular to this. The curvature of the tail is traced along maximum intensity (right panel) by angle-distance-vectors (α_i , d_i).

Table 2. Initial parameters of the two identical galaxies in the system of units suitable for 3C 48. Each galaxy consists of a spherical non-rotating bulge, a rotating exponential disk, and an isothermal halo (Hernquist 1993).

Parameter	Bulge	Disk	Halo
number of particles	8,000	8,000	8,000
softening length [kpc]	0.21	0.28	1.4
mass [$10^{10} M_\odot$]	1.86	5.60	32.48
scale length [kpc]	0.88	3.50	35.0
maximum radius [kpc]	7.0	52.5	105.0
scale height [kpc]		0.7	
maximum height [kpc]		7.0	

3. The 3C 48 look-alike

Different mass ratios of the initial galaxies, different snapshots during the merger process, and different projection angles of the merger remnants were probed in a still limited parameter study.

The nearest 3C 48 look-alike is found for the merger of two identical galaxies whose physical and numerical properties are given in Table 2. With these parameters the galaxies are similar to spirals of type Sb. The experimental setup is the same as used for simulations of the "Antennae" – i.e. both galaxies are symmetrically oriented with $i_1 = i_2 = 60^\circ$ and $\omega_1 = \omega_2 = -30^\circ$ (see Toomre & Toomre 1972; Barnes 1988). The model galaxies are initialized near the apocentre of the corresponding elliptical Keplerian orbit which is defined by the eccentricity of $e = 0.5$, the pericentric distance of $r_{\text{peri}} = 20$ kpc, and the period of 1.2 Gyr. The time step in the simulations is fixed to 1 Myr which guarantees that energy is conserved to better than 1% during the merger. The true decaying orbit is characterized by the generalized eccentricity of $e = 0.8$ and the pericentric distance of $r_{\text{peri}} = 7$ kpc. The outer regions of the two galaxy bulges begin to merge after ~ 272.5 Myr, just before pericentric passage. The merging is not a single process but the centres of the two bulges are repeatedly flung apart before they settle down in one common density peak.

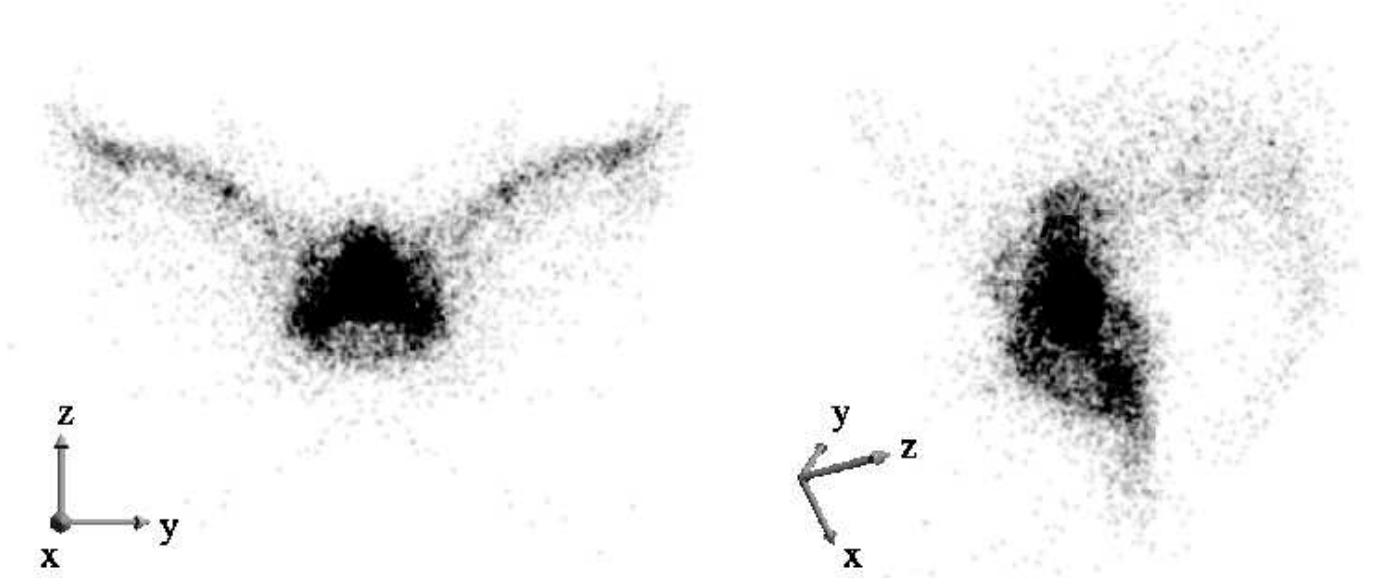


Fig. 2. Two different projections of the same simulation snapshot after 461.1 Myr. The left panel shows the projection for which the merger remnant looks like the "Antennae", the right panel shows the projection for which the remnant looks like the 3C 48 host. The coordinate planes indicate the respective tilt of the orbital plane (x-y). See text for a detailed description.

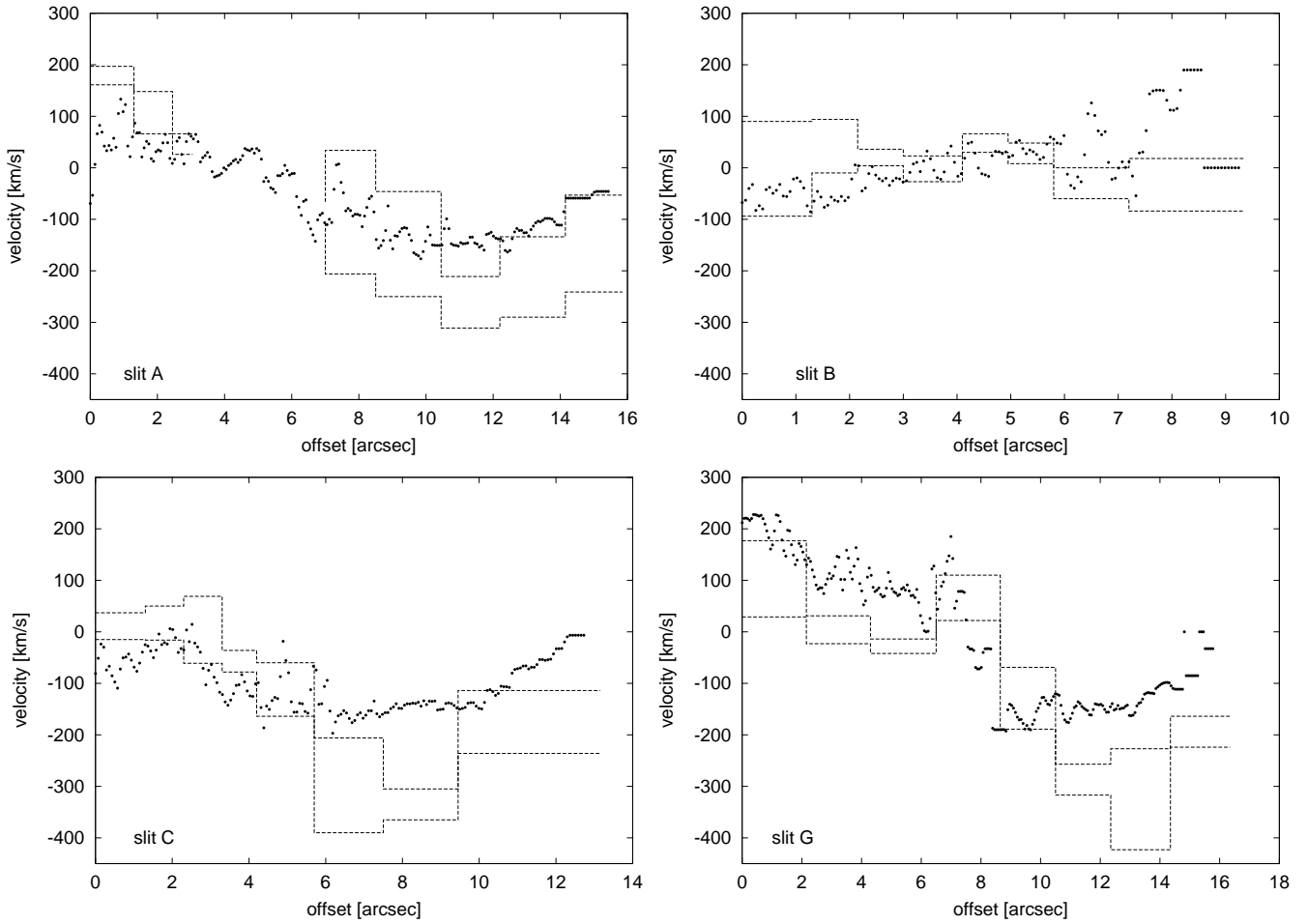


Fig. 4. Comparison of the observed and simulated line-of-sight velocities v_{LOS} along the four slits A, B, C, G. Offsets are measured in the direction indicated by the arrows in Fig. 3. Dots represent the average velocities of the 3C 48 look-alike. The area enclosed by $v_{\text{LOS}} + \Delta v_{\text{LOS}}$ and $v_{\text{LOS}} - \Delta v_{\text{LOS}}$ (dashed histograms) corresponds to the confidence region of the stellar line-of-sight velocities measured for the 3C 48 host. These data are taken from Fig. 1 and Table 2 in Canalizo & Stockton (2000).

Table 3. Measured proportions of the 3C 48 host, as taken from the contour plot in Fig. 1 of Canalizo & Stockton (2000), compared to the proportions of the nearest look-alike.

Ratios	3C 48 host	Look – alike
$L1/L2$	0.76	0.70
$L1/W1$	1.25	1.44
$L1/W2$	1.67	1.86
$L1/D$	0.52	0.55
$L2/W1$	1.65	2.06
$L2/W2$	2.20	2.64
$L2/D$	0.69	0.79
$W1/W2$	1.33	1.29
$W1/D$	0.42	0.38
$W2/D$	0.31	0.30

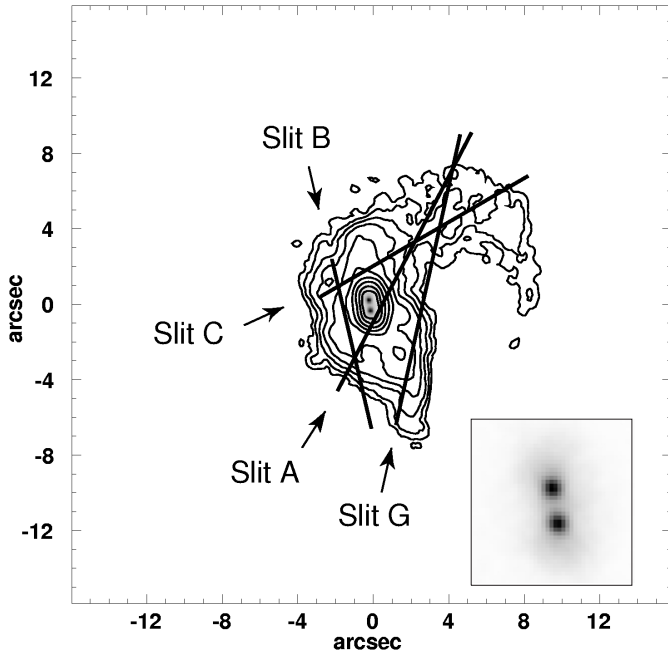


Fig. 3. Contour plot of the surface brightness of the 3C 48 look-alike. Length units are fixed in arcsec by positioning the four slits A, B, C, G used by Canalizo & Stockton (2000). The small inset shows a magnified view on the still separated density peaks of the merging bulges.

The nearest 3C 48 look-alike emerges after 461.1 Myr. Two projections of this merger remnant are shown in Fig. 2. In the left panel (“Antennae” look-alike), the view is perpendicular to the orbital plane x - y . In the right panel, (3C 48 look-alike) the orbital plane is tilted southwards, westwards, and counterclockwise by 120° , 160° , and 116° , respectively. The proportions of the 3C 48 look-alike are listed in the right column of Table 3. The positions of the four slits A, B, C, G on the look-alike host and the resulting physical coordinate system are shown in Fig. 3. In Fig. 4, the scaled velocities along the slits are compared to the confidence region of stellar line-of-sight velocities given for 3C 48 by Canalizo & Stockton (2000). The angle-versus-distance comparison for the curvature of the northwestern tidal tail is shown in Fig. 5.

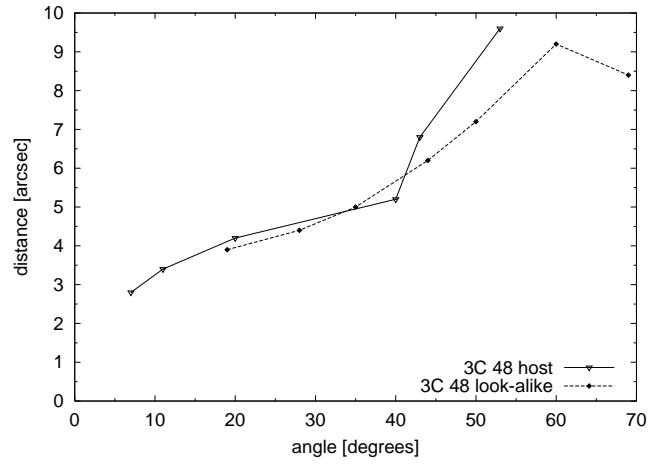


Fig. 5. Comparison of the curvature of the northwestern tidal tail of the 3C 48 host (solid line) and its look-alike (dashed line).

4. Discussion

4.1. The nature of 3C 48A

Optical and near-infrared images of the 3C 48 host show two luminosity peaks at the positions of 3C 48 and 3C 48A, the latter being located about $1''$ northeast of 3C 48 (e.g. Stockton & Ridgway 1991; Canalizo & Stockton 2000). With softening lengths of ~ 0.25 kpc ($0''.06$) for the bulge and disk particles (see Table 2), the spatial resolution of the simulations is high enough to identify corresponding density peaks in the 3C 48 model. As shown in the small inset in Fig. 3, the centres of the bulge components of the two merging galaxies are still separated at the stage of the 3C 48 look-alike. Their distance of about $0''.6$ (2.5 kpc) and their relative positions on a southwestern to northeastern axis are similar to the observed configuration of 3C 48 and 3C 48A. Thus, a scenario with 3C 48 and 3C 48A being the two centres of merging galaxies is possible. However, the exact configuration of the density peaks in the simulations is very sensitive to the projection angle and to the time at which the snapshot is taken. About 20 Myr later, the two peaks have already merged into one. Furthermore, the purely stellar-dynamical model does not address the question of a possible nuclear activity at the positions of 3C 48 and 3C 48A. A detailed discussion of nuclear activity depends on whether or not a black hole exists at the mentioned positions and on the respective fueling rates.

4.2. Location of the counter tidal tail

Since each of the two merging disk galaxies forms a tidal tail, the missing second tidal tail has always been a caveat of the merger hypothesis for 3C 48. Here, the simulations suggest a simple solution: At the projection angle of the 3C 48 look-alike, the second tidal tail is mainly located in front of the body of the host and, therefore, severely foreshortened. It extends from the southwest towards the northeast, roughly along slit B, so that measurements along this slit trace a mixture of line-of-sight velocities from the body and from the tail. This could explain why the observed and the simulated line-of-sight velocity sig-

natures along slit B (Fig. 4) are dominated by scattering around a mean velocity close to zero. Slits A, C, and G, in contrast, are characterized by large absolute line-of-sight velocities (up to ~ 200 to 300 km s^{-1}) and strong variations along the slits. A counter tidal tail extending from the southwest towards the northeast in front of the main body of the 3C 48 host is a completely new alternative. Regarding the information about stellar kinematics, this location seems to be more likely than the two suggested tails in the southeast and from the southeast towards the southwest (Boyce et al. 1999; Canalizo & Stockton 2000) which have failed identification so far.

4.3. The evolutionary history of 3C 48

Conclusions about the orbital parameters for 3C 48 and the original parameters of the merging galaxies can only be tentative. The orbital period of the best fit model amounts to about 20% of the age of the universe at the redshift of 3C 48 ($\sim 5.4 \text{ Gyr}$). A merger scenario with such an orbital period is plausible, assuming an initially highly eccentric orbit of the merging galaxies which is transformed into a bound orbit by dynamical friction of their dark matter halos (e.g. Jones & Stein 1989). It has been found that the morphology and the kinematics of tidal tails are very sensitive to the rotation curve of the interacting model galaxies (Dubinski et al. 1996; Mihos et al. 1998; Dubinski et al. 1999). Thus, instead of two identical galaxies, an alternative model for 3C 48 could start from two galaxies with different rotation curves so that only one of them forms an extended tidal tail. However, even in its generality the multi-particle model presented in this paper gives rather compelling evidence that the formation of 3C 48 is linked to a merger process. Therewith, 3C 48 ranks among these transitional objects which support the evolutionary scenario (Sanders et al. 1988) in its original merger-driven definition.

References

- Barkhouse, W. A. & Hall, P. B. 2001, *AJ*, 121, 2843
 Barnes, J. E. 1988, *ApJ*, 331, 699
 Boroson, T. A. & Oke, J. B. 1982, *Nature*, 296, 397
 Boyce, P. J., Disney, M. J., & Bleaken, D. G. 1999, *MNRAS*, 302, L39
 Canalizo, G. & Stockton, A. 2000, *ApJ*, 528, 201
 Chatzichristou, E. T., Vanderriest, C., & Jaffe, W. 1999, *A&A*, 343, 407
 Dubinski, J., Mihos, J. C., & Hernquist, L. 1996, *ApJ*, 462, 576
 —. 1999, *ApJ*, 526, 607
 Hernquist, L. 1993, *ApJS*, 86, 389
 Hernquist, L. & Katz, N. 1989, *ApJS*, 70, 419
 Jones, B. & Stein, W. A. 1989, *AJ*, 98, 1557
 Ma, C., Arias, E. F., Eubanks, T. M., et al. 1998, *AJ*, 116, 516
 Matthews, T. A., Bolton, J. G., Greenstein, J. L., Munch, G., & Sandage, A. R. 1961, *Sky and Telescope*, 21, 148
 Matthews, T. A. & Sandage, A. R. 1963, *ApJ*, 138, 30
 Mihos, J. C., Dubinski, J., & Hernquist, L. 1998, *ApJ*, 494, 183
 Neugebauer, G., Soifer, B. T., & Miley, G. K. 1985, *ApJ*, 295, L27

- Sanders, D. B., Soifer, B. T., Elias, J. H., et al. 1988, *ApJ*, 325, 74
 Scoville, N. Z., Padin, S., Soifer, B. T., Yun, M. S., & Sanders, D. B. 1993, *Bulletin of the American Astronomical Society*, 25, 1241
 Stockton, A. & Ridgway, S. E. 1991, *AJ*, 102, 488
 Toomre, A. & Toomre, J. 1972, *ApJ*, 178, 623
 Wilkinson, P. N., Tzioumis, A. K., Benson, J. M., et al. 1991, *Nature*, 352, 313
 Wink, J. E., Guilloteau, S., & Wilson, T. L. 1997, *A&A*, 322, 427

Acknowledgements. Our special thanks go to Prof. Dr Lars Hernquist who kindly provided the codes TREESPH and BUILDGAL and gave helpful advice. This project was supported in part by the Deutsche Forschungsgemeinschaft (DFG) via grant SFB 494. J. Scharwächter is supported by a scholarship for doctoral students of the Studienstiftung des deutschen Volkes.